*AMSE JOURNALS –2014-Series: MODELLING B; Vol. 83;N° 1; pp 18-35*
*Submitted April 2013; Revised Dec. 26, 2013; Accepted Feb. 3, 2014*

# Ionized Micropolar Fluid Flow through a Vertical Plate

N. N. Anika, Tanvir Ahmed, D. Yasmin, F. Amin, and *Md. Mahmud Alam

Mathematics Discipline, Science, Engineering and Technology School
Khulna University, Khulna-9208, Bangladesh
(*alam_mahmud2000@yahoo.com, alam_mahmud2013@ku.ac.bd)

**Abstract :** The ionized micropolar fluid flow with heat and mass transfer over a vertical plate under the action of transverse magnetic field has been investigated numerically for the case of small magnetic Reynolds number. To obtain the non-similar non-dimensional momentum, energy and concentration equations, the usual non-dimensional transformations have been used. The obtained equations are solved numerically by explicit finite deference method. The effects of various parameters on primary and secondary velocities, angular velocity, temperature and concentration as well as local and average shear stresses, Couple stress, Nusselt number and Sherwood number are shown in graphically. Finally, a qualitative comparison with previous work has been tabulated.

## Key words
Ionized Fluid, Micropolar Fluid, Heat And Mass Transfer, Finite Difference Method.

## 1. Introduction

Partially ionized plasma is usually described by a single-fluid particle approach, where the ion-neutral collision effects are expressed by Cowling (1957) conductivity in the induction equation. In the course of this decade, efforts have been made to extend the Magnetomicropolar phenomena subject to an external magnetic field. Micropolar fluids are fluids with microstructure belonging to a class of fluids with nonsymmetrical stress tensor referred to as polar fluids. Physically, they represent fluids consisting of randomly oriented particles suspended in a viscous medium, and they are important to engineers and scientists working with hydrodynamic-fluid problems. Micropolar Fluids is an essential resource for anyone wishing to

understand and needing to use concepts and methods when working with the hydrodynamics of miropolar fluids. The magnetohydrodynamic flow between two parallel plates, known as Hartmann flow, is a classical problem that has many applications in MHD power generators, MHD pumps, accelerators, aerodynamic heating, electrostatic precipitation, polymer technology, petroleum industry, purification of crude oil and fluid droplets and sprays. A lot of research works concerning the Hartmann flow have been obtained under different physical effects. In most cases the Hall and Ion-slip terms were ignored in applying Ohm's law as they have no marked effect for small and moderate values of the magnetic field. However, the current trend for the application of MHD is towards a strong magnetic field, so that the influence of electromagnetic force is noticeable. Under these conditions, the Hall current and Ion-slip are important and they have a marked effect on the magnitude and direction of the current density and consequently on the magnetic force term. Free convection flows are studied because of their wide applications and hence it has attracted the attention of numerous investigators. Literature on heat and mass flux with ion-slip currents are very extensive due to its technical importance in the scientific community. When the conducting fluid is partially ionized-gas i.e. water gas seeds with potassium, the Hall and Ion-slip current are also significant. Sattar and Alam (1994) presented unsteady free convection and mass transfer flow of a viscous, incompressible and electrically conducting fluid past a moving infinite vertical porous plate with thermal diffusion effect.

The heat transfer problem associated with the boundary layer saturated fluid under different physical conditions has been studied by several authors. The diffusion of a chemical reactive species from a stretching sheet has been considered by Takhar et al. (2002).

The effects of Hall and Ion-slip currents on free convective heat generating flow in a rotating fluid have been studied by Ram (1995). It has been analyzed by Mittal and Bhat (1979) that discussed the forced convective heat transfer in a MHD channel with Hall and Ion-slip currents. Desseaux and Kelson (2000) studied the flow of a micropolar fluid bounded by a stretching sheet. In all the above studies, the authors took the stretching sheet to be oriented in horizontal direction. Abo-Eldahab, and Ghonaim (2003) investigated convective heat transfer in an electrically conducting micropolar fluid at a stretching surface with uniform free stream. The

Micropolar fluid behaviours on unsteady MHD heat and mass transfer flow with constant heat and mass fluxes with joule heating and viscous dissipation has been studied by Haque and Alam (2011). The effects of Hall and Ion-slip currents on free convective heat transfer flow past a vertical plate have been investigated by Ferdows et al. (2011).

The effects of chemical reaction, Hall and ion-slip currents on the MHD flow of a micropolar fluid through a porous medium have been analyzed by Mosta and Shateyi (2011) using the successive linearization method.

The objective of this study is to extend the work of Mosta and Shateyi (2011) with MHD forced convection heat and mass transfer fluid flow over a vertical plate. The problem has been solved by explicit finite difference method. The governing equations involved in this problem have been transformed into non-similar coupled partial differential equation by usual transformations. Finally, the comparison of the present results with the results of Mosta and Shateyi (2011) has been shown in tabular form.

## 2. Mathematical Formulation

Consider an unsteady MHD electrically conducting incompressible viscous micropolar fluid flow past over a vertical electrically nonconducting isothermal plate in the presence of traverse magnetic field $B_0$ in vector form $\mathbf{B} = (0, B_0, 0)$. The fluid flow is also assumed to be in the x -direction which is taken along the plate in the upward direction and y -axis is normal to it. Initially the fluid as well as the plate is at rest and it is considered that the plate as well as the fluid is at the same temperature $T(= T_\infty)$ and concentration level $C(= C_\infty)$. Also it is assumed that the temperature of the plate and spices concentration are raised to $T_w(> T_\infty)$ and $C_w(> C_\infty)$ respectively, which are there after maintained constant, where $T_w, C_w$ are temperature and spices concentration at the wall and $T_\infty, C_\infty$ are the temperature and concentration of the species outside the plate respectively. The physical configuration of the problem is furnished in **Fig. 1.**

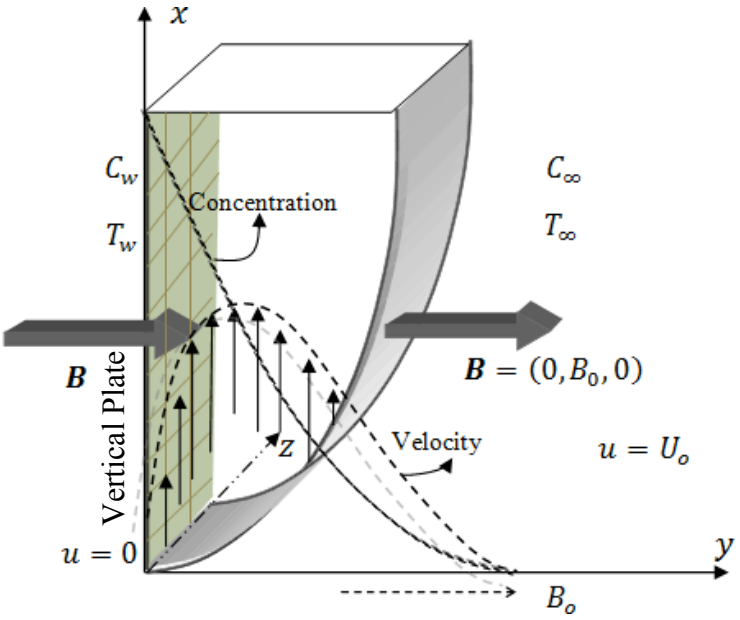


Fig. 1. Physical configuration and coordinate system.

The magnetic Reynolds number of the flow is taken to be small enough field and the magnetic field is negligible in comparison with applied magnetic field and the magnetic lines are fixed relative to the fluid. Using the relation $\nabla \cdot \mathbf{J} = 0$ for the current density $\mathbf{J} = (J_x, J_y, J_z)$ where $J_y = \text{constant}$. Since the plate is non-conducting, $J_y = 0$ at the plate and hence zero everywhere. The generalized Ohm's law in the absence of electric field to the case of short circuit problem (T. G. Cowling (1956));

$$\mathbf{J} = \sigma\left(\mathbf{q} \wedge \mathbf{B} + \frac{1}{ne} grad\, p_e\right) - \frac{\beta_e}{H_0}(\mathbf{J} \wedge \mathbf{B}) + \frac{\beta_i \beta_e}{H_0}(\mathbf{J} \wedge \mathbf{B}) \wedge \mathbf{B}$$

where $\sigma, \mu_e, n, e, p_e, \beta_e$ and $\beta_i$ are the electric conductivity, the magnetic permeability, the number of density of electron, the electric charge, the electron pressure, Hall parameter, and Ion-slip parameter, respectively. If we neglect the electron pressure, we have

$$J_x = \frac{\sigma B_0}{\alpha_e^2 + \beta_e^2}(u\beta_e - w\alpha_e), \quad J_z = \frac{\sigma B_0}{\alpha_e^2 + \beta_e^2}(w\beta_e + u\alpha_e)$$

where $\alpha_e = 1 + \beta_i \beta_e$

The above mentioned framework generalized under the usual boundary layer approximation, the governing equation in two dimensional systems under consideration can be written as:

Continuity equation;

$$\frac{\partial u}{\partial x} + \frac{\partial v}{\partial y} = 0 \tag{1}$$

Momentum equations;

$$\frac{\partial u}{\partial t}+u\frac{\partial u}{\partial x}+v\frac{\partial u}{\partial y}=g\beta_T\left(T-T_\infty\right)+g\beta_C\left(C-C_\infty\right)+\left(\upsilon+\frac{\chi}{\rho}\right)\left(\frac{\partial^2 u}{\partial y^2}\right)+\frac{\chi}{\rho}\frac{\partial N}{\partial y}$$

$$-\frac{1}{\rho}\frac{\sigma {B_0}^2}{\left({\alpha_e}^2+{\beta_e}^2\right)}\left[\alpha_e u+\beta_e w\right] \quad (2)$$

$$\frac{\partial w}{\partial t}+u\frac{\partial w}{\partial x}+v\frac{\partial w}{\partial y}=\left(\upsilon+\frac{\chi}{\rho}\right)\left(\frac{\partial^2 w}{\partial y^2}\right)+\frac{1}{\rho}\frac{\sigma {B_0}^2}{\left({\alpha_e}^2+{\beta_e}^2\right)}\left[\beta_e \mathrm{u}-\alpha_e \mathrm{w}\right] \quad (3)$$

Angular Momentum;

$$\frac{\partial N}{\partial t}+u\frac{\partial N}{\partial x}+v\frac{\partial N}{\partial y}=\frac{\gamma}{\rho j}\left(\frac{\partial^2 N}{\partial y^2}\right)-\frac{\chi}{\rho j}\frac{\partial u}{\partial y}-2\frac{\chi}{\rho j}N \quad (4)$$

Energy equation;

$$\frac{\partial T}{\partial t}+u\frac{\partial T}{\partial x}+v\frac{\partial T}{\partial y}=\frac{\kappa}{\rho c_p}\left(\frac{\partial^2 T}{\partial y^2}\right)+\frac{1}{c_p}\left(\upsilon+\frac{\chi}{\rho}\right)\left\{\left(\frac{\partial u}{\partial y}\right)^2+\left(\frac{\partial w}{\partial y}\right)^2\right\}$$

$$+\frac{\sigma {B_0}^2}{\rho c_p\left({\alpha_e}^2+{\beta_e}^2\right)}\left[w^2+u^2\right] \quad (5)$$

Concentration equation;

$$\frac{\partial C}{\partial t}+u\frac{\partial C}{\partial x}+v\frac{\partial C}{\partial y}=D\left(\frac{\partial^2 C}{\partial y^2}\right) \quad (6)$$

with the corresponding boundary conditions are;

$$u=0,v=0,w=0,N=-S\frac{\partial u}{\partial y},\ T=T_w,C=C_w \text{ at } y=0 \quad (7)$$

$u=0,\ v=0,\ w=0,\ N=0,\ T\to 0,\ C\to 0$ as $y\to\infty$

where $u$, $v$ and $w$ are the $x$, $y$ and $z$ components of velocity vector, $\sigma$ is the electric conductivity, $\upsilon$ is the kinematic coefficient viscosity, $\rho$ is the density of the fluid, $\kappa$ is the thermal conductivity, $c_p$ is the specific heat at the constant pressure , $D$ is the coefficient of mass diffusivity, $\beta_T$ is the co-efficient of volumetric expansion for heat transfer, $\beta_C$ is the co-efficient of volumetric expansion for mass transfer, respectively. And $s$ be an arbitrary constant. When $s=0$, it has been found that $N=0$, which represents no-spin condition i.e., the microelements in a concentrated particle flow close to the wall are not able to rotate. The case $s=\frac{1}{2}$ represents vanishing of the anti-symmetric part of the stress tensor and represents weak concentration. In a fine particle suspension of the particle spin is equal to the fluid velocity at the wall. The case $s=1$ represents turbulent boundary layer flow.

To obtain the governing equations and the boundary condition in dimension less form, the following no-dimensional quantities are introduced as;

$X = \frac{xU_0}{\upsilon}$, $Y = \frac{yU_0}{\upsilon}$, $U = \frac{u}{U_0}$, $V = \frac{v}{U_0}$, $W = \frac{w}{U_0}$, $\tau = \frac{tU_\infty^2}{\upsilon}$, $\Omega = \frac{N\upsilon}{U_0^2}$ $\theta = \frac{T - T_\infty}{T_w - T_\infty}$ and

$\Phi = \frac{C - C_\infty}{C_w - C_\infty}$

Using the above non-dimensional variables in equations (1)-(6) and corresponding boundary conditions (6), the following equations are obtained as:

$$\frac{\partial U}{\partial X} + \frac{\partial U}{\partial Y} = 0 \tag{8}$$

$$\frac{\partial U}{\partial T} + U\frac{\partial U}{\partial X} + V\frac{\partial U}{\partial Y} = (1 + \Delta)\left(\frac{\partial^2 U}{\partial Y^2}\right) + \Delta\frac{\partial \Gamma}{\partial Y} + G_r\theta + G_r^*\Phi - \frac{M}{(\alpha_e^2 + \beta_e^2)}\left[\alpha_e U + \beta_e W\right] \tag{9}$$

$$\frac{\partial W}{\partial T} + U\frac{\partial W}{\partial X} + V\frac{\partial W}{\partial Y} = (1 + \Delta)\left(\frac{\partial^2 W}{\partial Y^2}\right) + \frac{M}{(\alpha_e^2 + \beta_e^2)}\left[\beta_e U - \alpha_e W\right] \tag{10}$$

$$\frac{\partial \Omega}{\partial T} + U\frac{\partial \Omega}{\partial X} + V\frac{\partial \Omega}{\partial Y} = \Delta\left(\frac{\partial^2 \Omega}{\partial Y^2}\right) - \lambda\left(2\Gamma + \frac{\partial U}{\partial Y}\right) \tag{11}$$

$$\frac{\partial \theta}{\partial \tau} + U\frac{\partial \theta}{\partial X} + V\frac{\partial \theta}{\partial Y} = \frac{1}{P_r}\frac{\partial^2 \theta}{\partial Y^2} + E_c(1 + \Delta)\left(\left(\frac{\partial U}{\partial Y}\right)^2 + \left(\frac{\partial W}{\partial Y}\right)^2\right) + M\frac{E_c}{(\alpha_e^2 + \beta_e^2)}\left[U^2 + W^2\right] \tag{12}$$

$$\frac{\partial \Phi}{\partial T} + U\frac{\partial \Phi}{\partial X} + V\frac{\partial \Phi}{\partial Y} = \frac{1}{S_c}\left(\frac{\partial^2 \Phi}{\partial Y^2}\right) \tag{13}$$

boundary conditions are;

$$U=0,\ V=0,\ W=0,\ \Omega = -S\frac{\partial U}{\partial Y},\ \theta = 1,\ \Phi = 1 \text{ at } Y = 0 \tag{14}$$

$$U = 0,\ V = 0,\ W = 0,\ \Omega = 0,\ \theta \to 0,\ \Phi \to 1 \text{ as } Y \to \infty$$

where $\tau$ represents the dimensionless time, $X$ and $Y$ are the dimensionless Cartesian coordinates, $U$ and $V$ is the dimensionless velocity component in $X$ and $Z$ direction, $\theta$ is the dimensionless temperature, $\Phi$ is the dimensionless concentration, $\Delta = \frac{\chi}{\rho\upsilon}$ (Microrotation parameter), $G_r = \frac{g\beta(T_w - T_\infty)\upsilon}{U_0^3}$ (Grashof Number), $G_r^* = \frac{g\beta^*(C_w - C_\infty)\upsilon}{U_0^3}$ (Modified Grashof Number), $M = \frac{B_0^2\sigma_e\upsilon}{\rho U_0^2}$ (Magnetic Parameter), $\Lambda = \frac{\gamma}{\rho j\upsilon}$ (Spin Gradient Viscosity), $\lambda = \frac{\chi\upsilon}{\rho j U_0^2}$

(Vortex Viscosity), $P_r = \frac{\rho c_p \upsilon}{\kappa}$(Prandlt Number), $E_c = \frac{U_o{}^2}{c_p(T_w - T_\infty)}$ (Eckert Number), $S_c = \frac{\upsilon}{D}$ (Schmidt number).

## 3. Shear Stresses, Couple Stresses, Nusselt Number and Sherwood Number

All The quantities of chief physical interest are shear stresses, couple stress, Nusselt number and Sherwood number. The following equations represent the local and average shear stresses at the plate local stress in $x$-direction, $\tau_{xL} = \mu_0 \left(\frac{\partial u}{\partial y}\right)_{y=0}$ and average shear stress in $x$-direction, $\tau_{xA} = \mu_0 \int \left(\frac{\partial u}{\partial y}\right)_{y=0} dx$ which are proportional to $\left(\frac{\partial U}{\partial Y}\right)_{Y=0}$ and $\int_0^{100} \left(\frac{\partial U}{\partial Y}\right)_{Y=0} dX$ respectively. The local Shear stress in $z$-direction, $\tau_{zL} = \mu_0 \left(\frac{\partial w}{\partial y}\right)_{y=0}$ and average shear stress in $z$-direction, $\tau_{zA} = \mu_0 \int \left(\frac{\partial w}{\partial y}\right)_{y=0} dx$ which are proportional to $\left(\frac{\partial W}{\partial Y}\right)_{Y=0}$ and $\int_0^{100} \left(\frac{\partial W}{\partial Y}\right)_{Y=0} dX$ respectively. From the Microrotation field, it has been investigated that the effects of various parameters on the local and average couple stress. The following equations represent the local and average couple stress at the wall, local couple stress $M_L = \frac{\upsilon j \rho}{\gamma} \left(\frac{\partial N}{\partial y}\right)_{y=0}$ and average couple stress $M_A = \frac{\upsilon j \rho}{\gamma} \int \left(\frac{\partial N}{\partial y}\right)_{y=0} dx$ which are proportional to $\left(\frac{\partial \Omega}{\partial Y}\right)_{Y=0}$ and $\int_0^{100} \left(\frac{\partial \Omega}{\partial Y}\right)_{Y=0} dX$ respectively. From the temperature field, it has been investigated the effects of various parameters on the local and average heat transfer coefficients. The following equations represent the local and average heat transfer rate that is well known Nusselt number, local Nusselt number, $N_{uL} = \left(\frac{\partial T}{\partial y}\right)_{y=0}$ and average Nusselt number, $N_{uA} = \int \left(\frac{\partial T}{\partial y}\right)_{y=0} dx$ which are proportional to $\left(\frac{\partial \theta}{\partial Y}\right)_{Y=0}$ and $\int_0^{100} \left(\frac{\partial \theta}{\partial Y}\right)_{Y=0} dX$ respectively. And from the concentration field, the following equations represent the local and average mass transfer rate that is well known Sherwood number, local Sherwood

number, $S_{hL} = \left(\frac{\partial C}{\partial y}\right)_{y=0}$ and average Nusselt number, $S_{hA} = \int \left(\frac{\partial C}{\partial y}\right)_{y=0} dx$ which are proportional to $\left(\frac{\partial \phi}{\partial Y}\right)_{Y=0}$ and $\int_0^{100} \left(\frac{\partial \phi}{\partial Y}\right)_{Y=0} dX$ respectively.

## 4. Numerical Technique

In this paper, the governing coupled non similar non-linear partial differential equations with the associated initial and boundary conditions have been solved. From the concept of the above discussion, for simplicity the explicit finite difference method has been used to solve equations (8)-(13) subject to the conditions given by (14). To obtain the difference equations the region of the flow is divided into a grid or mesh of lines parallel to $X$ and $Y$ axes where $X$-axis is taken along the plate and $Y$-axis is normal to the plate.

Here the plate of height $X_{\max}(=100)$ is considered i.e. $X$ varies from 0 to 100 and assumed $Y_{\max}(=25)$ as corresponding to $Y \to \infty$ i.e. $Y$ varies from 0 to 25. There are $m(=100)$ and $n(=100)$ grid spacing in the $X$ and $Y$ directions respectively as shown in **Fig. 2**. It is assumed that $\Delta X$, $\Delta Y$ are constant mesh size along $X$ and $Y$ directions respectively and taken as follows, $\Delta X = 1.00(0 \le X \le 100)$ and $\Delta Y = 0.25(0 \le Y \le 25)$ with the smaller time-step, $\Delta\tau = 0.005$.

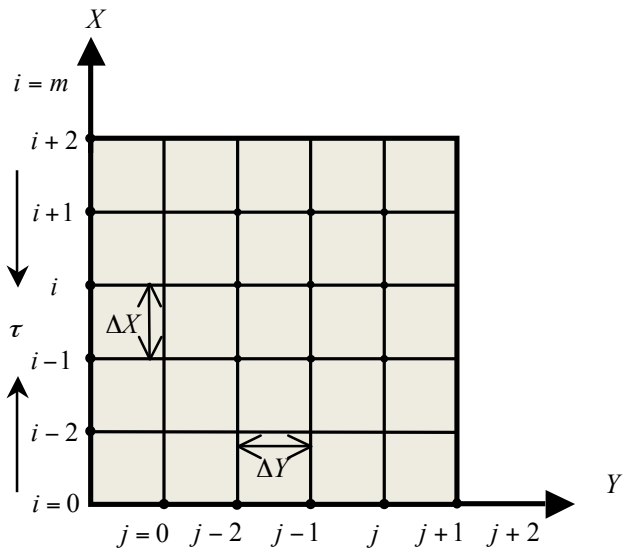


**Fig. 2.** Explicit finite difference grid system.

Let $U', V', W', \Omega', \theta'$ and $\Phi'$ denote the values of $U, V, W, \Omega, \theta$ and $\phi$ at the end of a time-step respectively. Using the explicit finite difference approximation we have an appropriate set of finite difference equations,

$$\frac{U_{i,j} - U_{i-1,j}}{\Delta X} + \frac{V_{i,j} - V_{i,j-1}}{\Delta Y} = 0 \tag{15}$$

$$\frac{U'_{i,j} - U_{i,j}}{\Delta\tau} + U_{i,j}\frac{U_{i,j} - U_{i-1,j}}{\Delta X} + V_{i,j}\frac{U_{i,j+1} - U_{i,j}}{\Delta Y} = (1+\Delta)\frac{U_{i,j+1} - 2U_{i,j} + U_{i,j-1}}{(\Delta Y)^2}$$

$$+ G_r\theta_{i,j} + \frac{\Gamma_{i,j+1} - \Gamma_{i,j}}{\Delta Y} - \frac{M}{\left(\alpha_e^{\,2} + \beta_e^{\,2}\right)}\left[\alpha_e U_{i,j} + \beta_e W_{i,j}\right] \tag{16}$$

$$\frac{W'_{i,j} - W_{i,j}}{\Delta\tau} + U_{i,j}\frac{W_{i,j} - W_{i-1,j}}{\Delta X} + V_{i,j}\frac{W_{i,j+1} - W_{i,j}}{\Delta Y} = (1+\Delta)\frac{W_{i,j+1} - 2W_{i,j} + W_{i,j-1}}{(\Delta Y)^2}$$

$$+ \frac{M}{\left(\alpha_e^{\,2} + \beta_e^{\,2}\right)}\left[\beta_e U_{i,j} - \alpha_e W_{i,j}\right] \tag{17}$$

$$\frac{\Omega'_{i,j} - \Omega_{i,j}}{\Delta\tau} + U_{i,j}\frac{\Omega_{i,j} - \Omega_{i-1,j}}{\Delta X} + V_{i,j}\frac{\Omega_{i,j+1} - \Omega_{i,j}}{\Delta Y} = \Lambda\frac{\Omega_{i,j+1} - 2\Omega_{i,j} + \Omega_{i,j-1}}{(\Delta Y)^2}$$

$$- \lambda\left(2\Omega_{i,j} + \frac{U_{i,j+1} - U_{i,j}}{\Delta Y}\right) \tag{18}$$

$$\frac{\theta'_{i,j} - \theta_{i,j}}{\Delta\tau} + U_{i,j}\frac{\theta_{i,j} - \theta_{i-1,j}}{\Delta X} + V_{i,j}\frac{\theta_{i,j+1} - \theta_{i,j}}{\Delta Y} = \frac{1}{P_r}\frac{\theta_{i,j+1} - 2\theta_{i,j} + \theta_{i,j-1}}{(\Delta Y)^2}$$

$$+ (1+\Delta)\left(\frac{U_{i,j+1} - U_{i,j}}{\Delta Y}\right)^2 + M\frac{E_c}{\left(a_e^2 + b_e^2\right)}\left(U_{i,j}^2 + W_{i,j}^2\right) \tag{19}$$

$$\frac{\Phi'_{i,j} - \Phi_{i,j}}{\Delta\tau} + U_{i,j}\frac{\Phi_{i,j} - \Phi_{i-1,j}}{\Delta X} + V_{i,j}\frac{\Phi_{i,j+1} - \Phi_{i,j}}{\Delta Y} = \frac{1}{S_c}\frac{\Phi_{i,j+1} - 2\Phi_{i,j} + \Phi_{i,j-1}}{(\Delta Y)^2} \tag{20}$$

with the boundary conditions;

$$U^n_{i,0} = 0,\ W^n_{i,0} = 0,\ \Omega^n_{i,0} = -s\frac{U^n_{i,1} - U^n_{i,0}}{\Delta Y},\ \theta^n_{i,0} = 1,\ \Phi^n_{i,0} = 1 \tag{21}$$

$U^n_{i,L} = 0,\ W^n_{i,L} = 0,\ \Omega^n_{i,L} = 0,\ \theta^n_{i,L} = 0, \Phi^n_{i,L} = 1$ where, $L \to \infty$

Here the subscript $i$ and $j$ designates the grid points with $X$ and $Y$ coordinates respectively and the superscript $n$ represents a value of time, $\tau = n\Delta\tau$ where $n = 0, 1, 2, \ldots\ldots$ .

The primary velocity $(U)$, secondary velocity $(W)$, Microrotation $(\Omega)$, temperature $(\theta)$ and concentration $(\Phi)$ distributions at all interior nodal points may be computed by successive applications of the above finite difference equations. The numerical values of the local shear stresses, local couple stress, local Nusselt number and local Sherwood number are evaluated by **Five-point** approximate formula for the derivatives and then the average Shear Stress, Couple stress, Nusselt number and Sherwood number are calculated by the use of the **Simpson's** $\frac{1}{3}$ integration formula. The stability conditions and the convergence criteria are not shown for brevity.

## 5. Results and Discussion

For the purpose of observing the Physical significance of the model, the approximate solutions are obtained for various parameters with small values of Eckert number $E_c$. In order to analyze the physical situation of the above model has been computed the numerical values of the primary velocity $U$, secondary velocity $W$, angular velocity $\Omega$, temperature $\theta$ and Concentration $\phi$ within the boundary layer for different values of dimensionless magnetic parameter $(M)$, Grashof number $(G_r)$, Modified Grashof number $(G_r^*)$, Prandtl number $(P_r)$, Spin gradient viscosity $(\Lambda)$, Microrotation number $(\Delta)$, Vortex viscosity $(\lambda)$, Hall current $(\beta_e)$, ion-slip parameter $(\beta_i)$, Schmidt number $(S_c)$, an arbitrary constant $(S)$ and Eckert number $(E_c)$. For Schmidt number $(S_c)$ the values 0.60, 0.95, 5.00 are considered, which represent specific condition of flow ($0.6$ corresponds to water vapor that represents the most common effect in air, $0.95$ belongs to carbon-di-oxide at temperature $25^0$ and 1 atmospheric pressure and $5.00$ corresponds to highly viscous fluid). To get the steady state solutions, the computations have been carried out upto dimensionless time $\tau = 80$. It has been observed that, results show visible change for the primary velocity $U$, secondary velocity $W$, angular velocity $\Omega$, temperature $\theta$ and Concentration $\Phi$ at dimensionless time $\tau = 5$ to $\tau = 30$. But in the case of dimensionless time $\tau = 31$ to $80$ has no visible changes. Thus the solutions for dimensionless time $\tau \geq 30$ are essentially steady-state.

The primary velocity $U$, secondary velocity $W$, microrotation $\Omega$, temperature $\theta$ and concentration $\Phi$ profiles have been shown in Figs. 3-22 for different values of $M, \beta_e, \beta_i, P_r, E_c, S_c, \Lambda, \lambda, \Delta, G_r, G_r^*$ and $S$ in case of cooling plate. The values of

$M$, $\beta_e$, $\beta_i$, $E_c$, $\lambda$, $\Delta$ are however chosen arbitrary. The results have been generalized in several cases. The effect of Magnetic parameter $M$ as well as the different values of time step $\tau$ for the primary velocity distribution has been represented in Fig. 3. In this figure the maximum primary velocity $U$ reduces near the plate in case of strong magnetic field and then the velocity become zero within short range for same values of $M$. As compared to $\tau$ the magnitude of primary velocity increases with the increase of $\tau$. In Fig. 4, the secondary velocity continuously increases for the increase of $M$ and finally leads to zero asymptotically. The effect of $M$ on the microrotation profile has been shown in Fig. 5. The family of curves has a tendency to be twisted. Initially the angular velocity increases for the increase of $M$ below the line $X = 0$. Far away from the plate it has grown up in the upper side of $X = 0$. Spirally the angular velocity begins to decrease with the increasing parameter $M$ and then approaches and enters the line $X = 0$. Fig. 6 depicts the solution curves of temperature increases with the increase of magnetic parameter $M$. It indicates that the wall receives more and more heat from the fluid as the parameter increases. This is due to the plate possessing infinite source of heat. But in Fig. 7, the magnitude of concentration profile increases with the increase of $\tau$ as well as increase of magnetic parameter.

Fig. 8 showed that the secondary velocity increases gradually with the increase of $\beta_e$ and obtain a maximum value thereafter the secondary velocity decreases rapidly to meet the line $X = 0$ with the same increasing values of $\beta_e$. The effect of Prandtl number on the velocity profiles has been represented in Figs. 9-10. It is observed that $U$ and $W$ both are reduces due to increasing parameter $P_r$. The usual stabilizing effect of the Prandtl number on the boundary layer is also evident in this figure. After a comprehensive survey it has been found that the Fig. 11 is given another family of curves for different values of $P_r$ which is more similar to the Fig. 5. It is observed from Fig. 11, the angular velocity increases within the interval $0 < Y < 0.4$ (approx.) with the increase of $P_r$, whereas for roughly after $Y \geq 0.5$ the velocity decreases with the increase of $P_r$. The temperature decreased gradually with the increase of $P_r$ and at the steady state it has an increasing tendency within the range $0 < Y < 0.3$ as illustrated in Fig. 12. The concentration profile has minor effects due to increase of $P_r$. At $\tau = 30$, the change appears and it is increasing. But the total concentration increases as $\tau$ increases illustrated in Fig. 13.

Figs. 14-15, the primary and secondary velocity increases with the increase of Schmidt number $S_c$. From Fig. 16, it has been analyzed that the angular velocity $\Omega$ has visible effects

with the increase of $S_c$. Initially $\Omega$ decreases near the plate and being spiral they increases for the increase of $S_c$ and meet the line $X = 0$.In Fig. 17, it is seen that increase of $S_c$ leads to an increase in concentration profile. This is due to plate possessing infinite source of heat in the leading edge.

On the other hand Fig. 18 has been shown the different flow pattern for angular velocity. It has changed its direction twice for the different increasing values of vortex viscosity. The angular velocity decreases rapidly near the plate (approx, $Y \le 0.25$). As time passed the velocity become twisted and became maximum. Then it monotonically decreases and entered to the line $X = 0$ with the increase of $\lambda$. The effect of $\Lambda$ on the angular velocity profile exhibits in Fig. 19. The family of curves has a tendency to be twisted. Initially the angular velocity increases for the increase of $\Lambda$ below the line $X = 0$. Far away from the plate it creates a pick in upper side of $X = 0$. After that the prominent velocity begins to decrease with the increasing parameter $\Lambda$ and finally become zero asymptotically. It has been observed from Fig. 20, temperature increases faster and then decreases simultaneously with the increase of $E_c$ to meet the line $X = 0$. The primary as well as temperature profiles exhibit the remarkable no-change with the variations of $\beta_i$ as observed from Figs. 21 and 22. It is observed that for different values of $\beta_i$, the pick values of velocity shift a little but they have no significant effects on the primary and secondary velocity in the $x$ and $z$- direction. Like before, temperature as no change as is seen in Fig. 22.

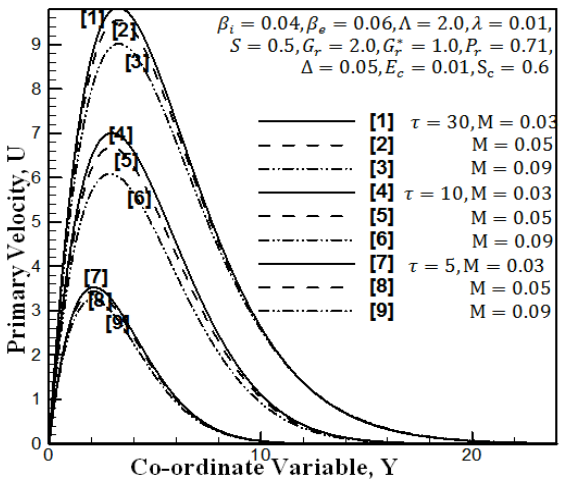


Fig.3. Primary velocity profiles for different values of Magnetic parameter, $M$ .

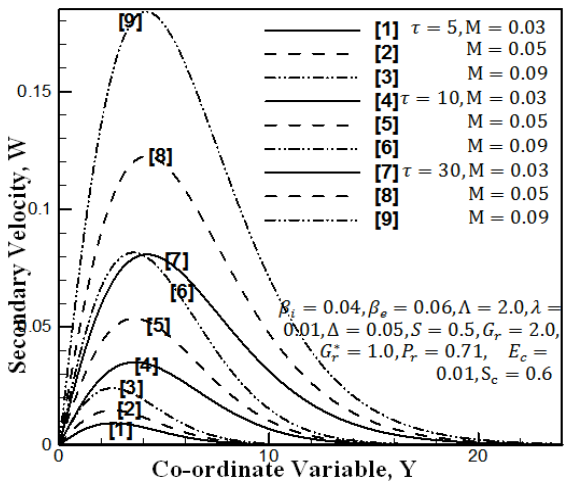


Fig.4. Secondary Velocity profiles for different values of Magnetic parameter $M$ .

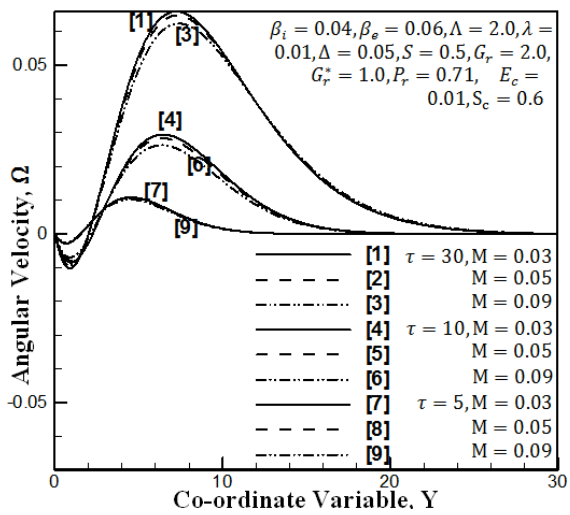


Fig.5. Microrotation profiles for different values of Magnetic parameter $M$ .

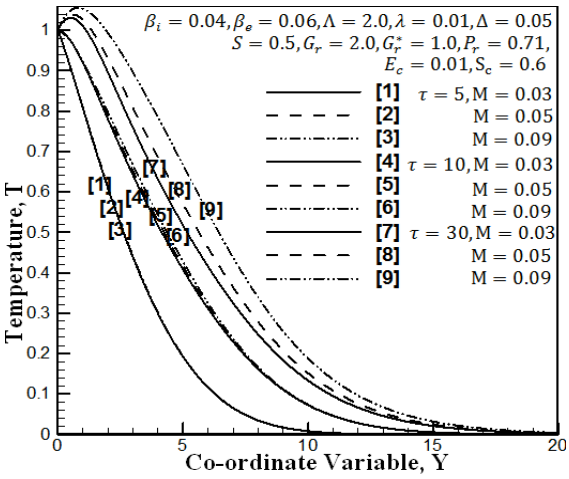


Fig.6. Temperature profiles for different values of Magnetic parameter $M$ .

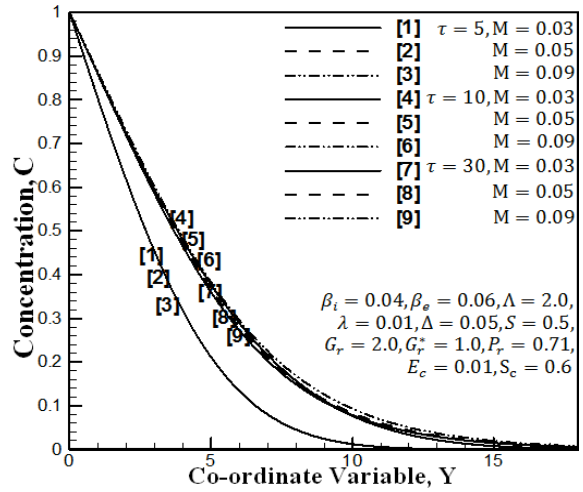


Fig.7. Concentration profiles for different values of Magnetic parameter $M$ .

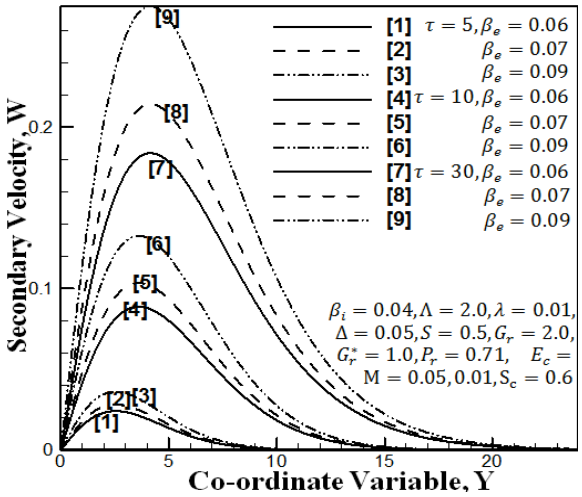


Fig.8. Secondary Velocity profiles for different values of Hall parameter $\beta_e$.

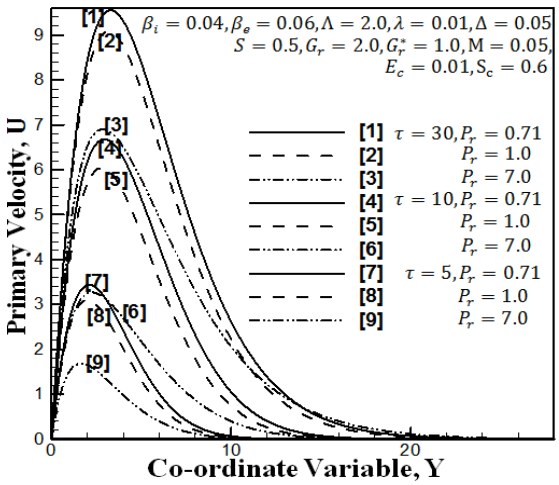


Fig.9. Primary velocity profiles for different values of Prandtl number $P_r$

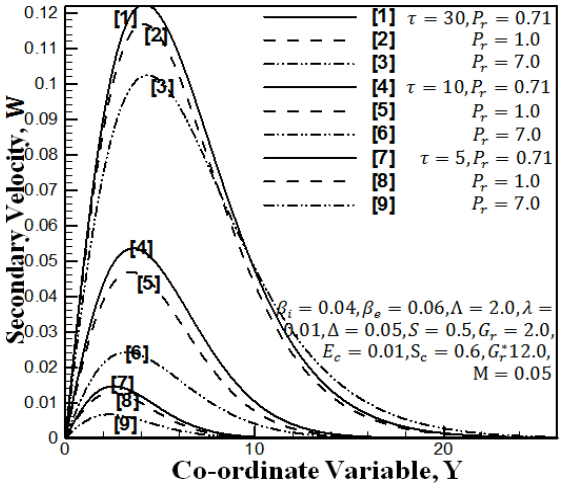


Fig.10. Secondary velocity profiles for different values of Prandtl number $P_r$

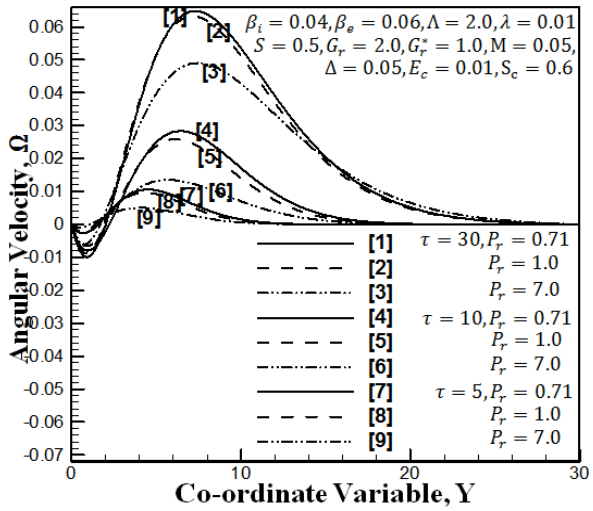


Fig.11. Microrotation profiles for different values of Prandtl number $P_r$

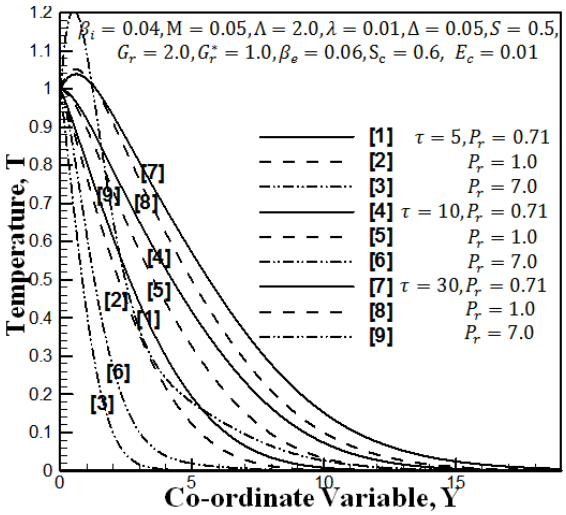


Fig.12. Temperature profiles for different values of Prandtl number $P_r$ .

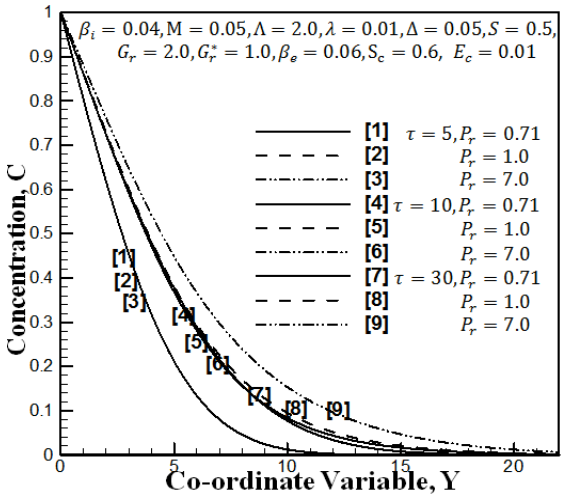


Fig.13. Concentration profiles for different values of Prandtl number $P_r$ .

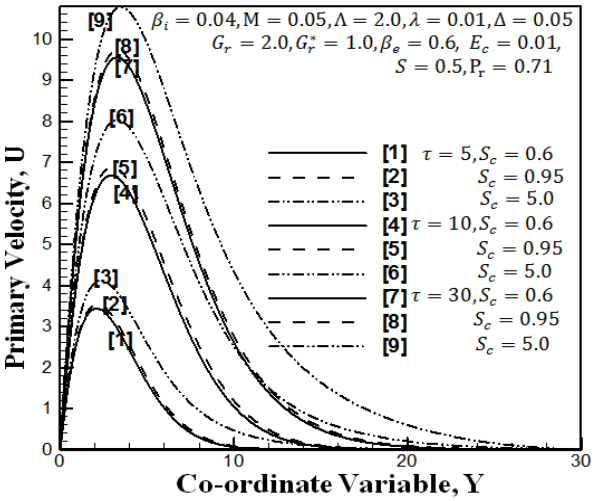


Fig.14. Primary velocity profiles for different values of Schmidt number $S_c$ .

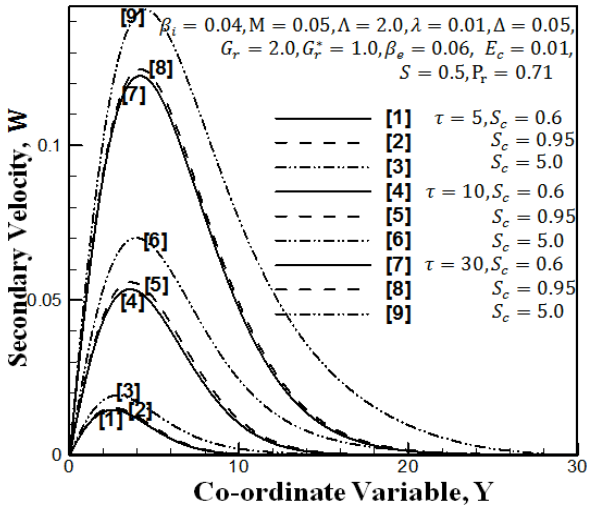


Fig.15. Secondary velocity profiles for different values of Schmidt number $S_c$ .

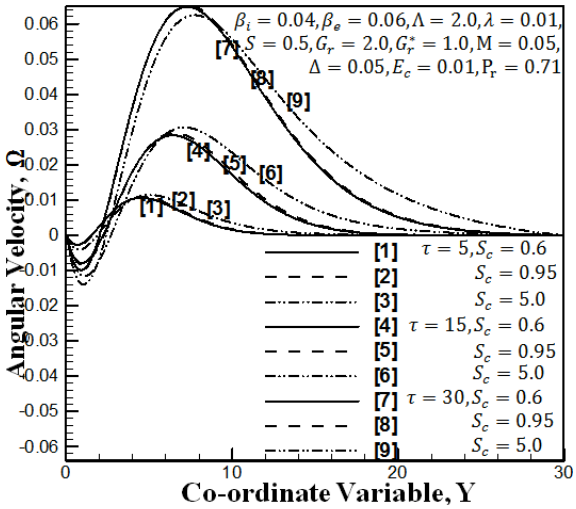


Fig.16. Microrotation profiles for different values of Schmidt number $S_c$ .

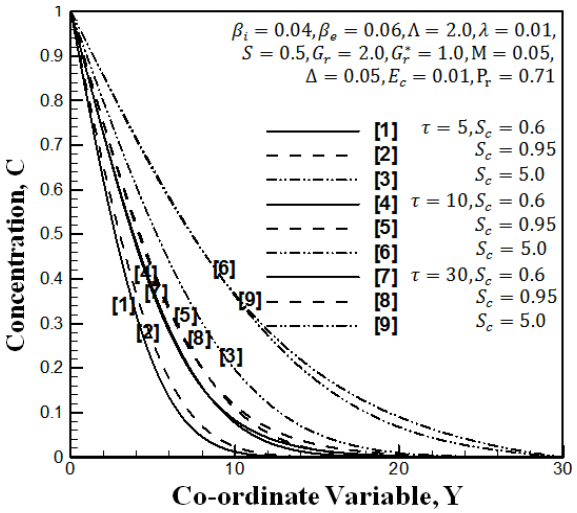


Fig.17. Concentration profiles for different values of Schmidt number $S_c$.

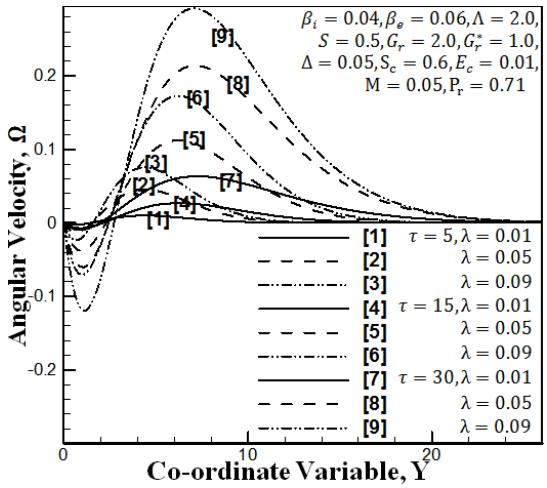


Fig.18. Microrotation profiles for different values of Vortex Viscosity $\lambda$.

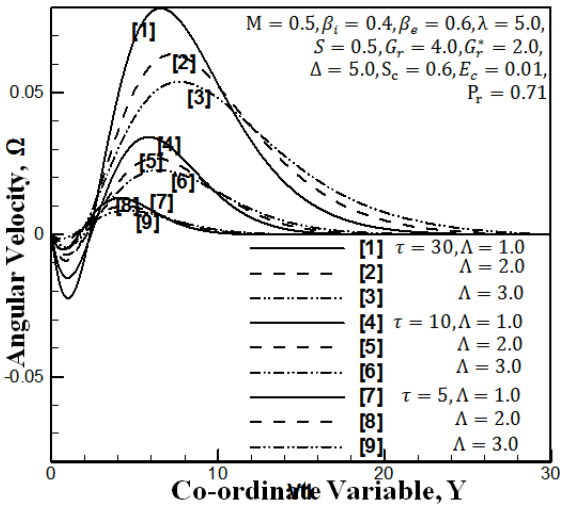


Fig.19. Microrotation profiles for different values of Spin Gradient Viscosity $\Lambda$.

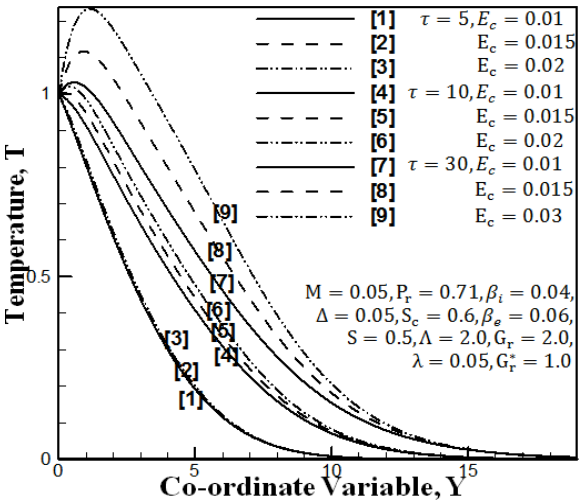


Fig.20. Temperature profiles for different values of dimensionless Eckert number $E_c$.

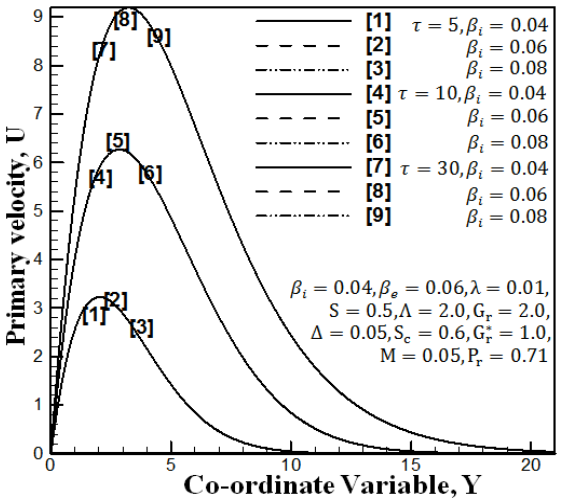


Fig.21. Primary velocity profiles for different values of Ion-slip parameter $\beta_i$.

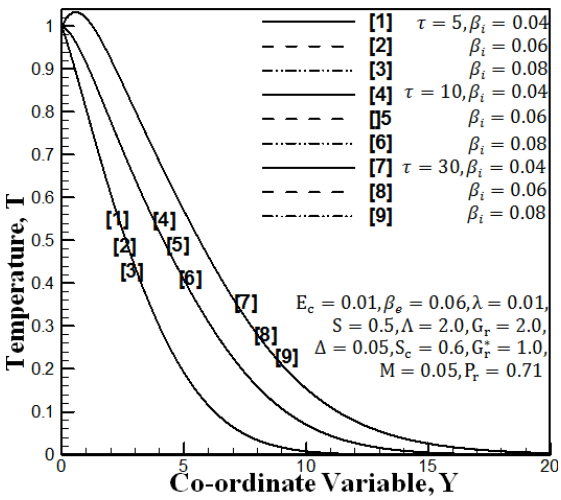


Fig.22. Temperature profiles for different values of Ion-slip parameter $\beta_i$.

## Conclusions

Unsteady MHD heat and mass transfer flow of an electrically conducting incompressible viscous fluid past a semi-infinite vertical plate under the action of usual magnetic flow for different fluid pattern is taken into account. The plate as well as the fluid is considered at the same temperature and the concentration label is same. The results are discussed for different values of important parameters as Prandtl number, Eckert number, Magnetic parameter, Vortex viscosity, Spin gradient Viscosity, Hall current, and Ion-slip current. The important findings of this model are very effective for any kind of change of parameters. The allover investigations considered graphically are listed below.

1. The primary velocity decreases with the increases of $M, P_r$ while the secondary velocity increases with the increase of $M, \beta_e, S_c$.
2. The secondary velocity decreases with the increase of $P_r$ while the primary velocity increases with the increase of $S_c$.
3. The angular velocity increases with the increase of $M, P_r \,\&\, \Lambda$ and the reverse effects found for the increase of $E_c, S_c \,\&\, \lambda$.
4. The temperature profile increases with the increase of $M, E_c$ while it decreases with the increase of $P_r$.
5. Concentration distribution increases with the increase of $M, P_r, \& S_c$.

The ion-slip parameter gives negligible effects as compared to Hall parameter due to usual magnetic field. The stability test is very effective and gives accurate result.

**Table 1. Qualitative comparison of the present results with the previous results**

| Increased Parameter | Previous results given by S.S.Mosta and S.Shateyi (2011) | | | | | Present results | | | | |
|---|---|---|---|---|---|---|---|---|---|---|
| | $f'(\eta)$ | $g(\eta)$ | $h(\eta)$ | $\theta(\eta)$ | $\phi(\eta)$ | $U$ | $W$ | $\Omega$ | $T$ | $C$ |
| $M$ | Dec. | Inc. | Dec | Inc. | Inc. | Dec. | Inc. | Inc. | Inc. | Inc. |
| $E_c$ | | | | Inc. | | | | Inc. | | |
| $S_c$ | | | | | | Inc. | Inc. | Dec. | Inc. | const |
| $\lambda$ | | . | | | . | const. | const. | Dec | cont. | const |
| $P_r$ | | | Inc. | | | Dec. | Dec. | Dec. | | |
| $\beta_e$ | Inc. | Dec. | Inc. | Dec. | Dec. | | Inc. | | | |
| $\beta_i$ | | Inc. | | | | const. | const | | . | |
| $\Lambda$ | | . | | | | . | . | Inc. | | |

## References


1. T. G. Cowling, "Magnetohydrodynamics", *Interscience Publications*, New York, 1957.
2. M. A. Sattar and M. M. Alam, "Thermal Diffusion as well as transpiration effects on MHD free convection and mass transfer flow past an accelerated vertical porous plate", *Indian Journal of pure applied Mathematics*, vol. 25, no. 6, pp. 679-688, 1994.
3. H. S. Takhar, A. J. Chamkha and G. Nath, "MHD flow over a moving plate in a rotating fluid with magnetic field hall currents and free stream velocity", *International Journal of Engineering Science*, vol. 40, no. 13, pp. 1511–1527, 2002.
4. P. C. Ram, "The Effect Hall and Ion-Slip Current on Free Convection Heat Generating Flow in a Rotating Fluid", *International journal of Energy Research*, vol. 19, no. 5, pp. 371-376, 1995.
5. M. L. Mittal and A. N. Bhat, "Forced convection Heat transfer in a MHD channel with Hall and Ion-slip current", *Applied Scientific Research*, vol. 35, no. 4, pp. 251-265, 1979.
6. A. Desseaux and N. A. Kelson, "Flow of a micropolar fluid bounded by a stretching sheet", *Anziam Journal,* vol. 42, no. E**,** pp.536-560, 2000.
7. E. M. Abo-Eldahab, and A. F. Ghonaim, "Convective heat transfer in an electrically conducting micropolar fluid at a stretching surface with uniform free stream", *Applied Mathematical Computations*, vol. 137, pp. 323-336, 2003.
8. M. Z. Haque and M. M. Alam, "Micropolar fluid behaviours on unsteady MHD heat and mass transfer flow with constant heat and mass fluxes, joule heating and viscous dissipation", *AMSE Journals (Modelling, Measurement and Control, Series B Mechanics and Thermics)*, vol. 80, no. 2, pp. 1-25, 2011.

9. M. Ferdows, , Esrat Jahan , M. A. A. Hamad, and Masahiro OTA , "Effects of Hall and ion-slip currents on free convective heat transfer flow past a vertical plate considering slip conditions", *Canadian Journal of Science and Engineering Mathematics*, vol. 2, no. 2, pp. 70-76, 2011.
10. S. S. Mosta and S. Shateyi, "The effects of chemical Reaction, Hall and Ion-slip currents on MHD Micropolar Fluid Flow with Thermal Diffusivity using a Novel Numerical Technique", *Journal of Applied Mathematics*, ID 689015, pp.30, 2011.